Front. Earth Sci. 2022, 16(2): 265–276
https://doi.org/10.1007/s11707-020-0841-1

RESEARCH ARTICLE

Research on vertical spatial characteristic of satellite infrared hyperspectral atmospheric sounding data

Ci SONG[1,2], Qiu YIN (✉)[3,4]

1 School of Communication and Information Engineering, Shanghai University, Shanghai 200444, China
2 College of Science, Zhongyuan University of Technology, Zhengzhou 450007, China
3 Shanghai Meteorological Service, Shanghai 200030, China
4 User Office of Meteorological Satellites, China Meteorological Administration, Shanghai 200030, China

Abstract Spatial characteristic is an important indicator of remote sensor performance, and space-borne infrared hyperspectral sounder is the frontier of atmospheric vertical sounding technology. In this paper, the formation mechanism of the vertical spatial characteristics involved in the space-borne infrared hyperspectral sounding data are analyzed in detail, which shows that the vertical spatial characteristics of sounding data depends not only on the spectral channels and their waveband coverage, but also the specific atmospheric parameter and its specific variation interested. The indicators of vertical spatial characteristics are defined and their mathematical models are established based on the mechanism analyses. These models are applied to the vertical spatial characteristic evaluation of atmospheric temperature sounding for FY-4A GIIRS, which is the first space-borne infrared hyperspectral atmospheric sounder in geostationary orbit. It is concluded that FY-4A GIIRS can sound the vertical temperature distribution in whole troposphere and lower stratosphere with height < 35 km. This study can provide basic information to support the improvement of infrared hyperspectral sounder and the trace of vertical spatial characteristics of atmospheric inversion products.

Keywords infrared hyperspectral, atmospheric sounding, vertical spatial characteristic, atmospheric temperature, FY-4A GIIRS

1 Introduction

Spatial characteristics of satellite remote sensing plays an important role in remote sensing performance. There are two meanings: one is the spatial characteristic of remote sensing data, and the other is the spatial characteristic of inversion product. The former is determined by remote sensing technology, while the latter is determined by remote sensing technology as well as remote sensing information processing methods.

The imager and the atmospheric vertical sounder are two typical satellite earth observing sensors. The former focuses on obtaining the horizontal images of atmospheric and earth surface features, and the latter focuses on obtaining the vertical distribution profiles of atmospheric parameters.

The spatial characteristics of imaging data usually refers to horizontal spatial characteristics described by pixel position, pixel size, pixel shape and the coverage of all pixels etc. It focuses on where the imager looks at, which depends on the imager's instantaneous field of view (FOV) and total FOV. Whether or not the target can be seen clearly by the imager is the concern of inversion product. So, the factors such as the strength of interested signal, the sensitivity of imager, and the solar radiation reflected by surface within instantaneous FOV, as well as the radiation of solar, atmosphere and surface outside instantaneous FOV which go into instantaneous FOV through atmospheric scattering, are all considered in the spatial characteristics evaluation of imaging inversion product, but not in the spatial characteristics evaluation of imaging data.

Therefore, if the spatial characteristics of imaging data are to be evaluated, the effecting factors will be simple and the effecting mechanism will be direct, in addition, the quantitative evaluating indicators will be easy to be determined. These indicators depend completely on the optical and mechanical design of imager, the design of satellite orbit and other geometric designs, and have nothing to do with the underlying surface parameters of concern (Niclòs et al., 2014; Qi, et al., 2016; Hu et al.,

Received August 13, 2020; accepted October 9, 2020

E-mail: yinqiu@cma.gov.cn

2018;Qi et al., 2019; Friedl et al., 2002). For example, the medium resolution spectral imager-II (MERSI-2) on board FY-3D, which is a polar-orbiting meteorological satellite launched in November 2017 with orbit altitude 836 km, applied 10/40-pixel detectors' parallel scanning and 45° scanning mirror having 1.2 mrd/0.3 mrd of instantaneous FOV and ±55.1° of the total FOV. It can be easy deduced that spatial resolution of FY-3D MERSI-2 at substellar point are 1000 m and 250 m respectively, and the image width is 2930 km (Hu et al., 2018). As for the spatial characteristics of inversion products obtained from imaging data, the inversion method such as sub-pixel decomposition technique has been studied extensively.

Atmospheric sounder detects the vertical distribution of physical parameters such as atmospheric temperature and humidity etc. For satellite infrared atmospheric sounder, from multispectral technology with filter (such as vertical temperature profile radiometer VTPR, high resolution infrared radiation sounder HIRS and infrared atmospheric sounder IRAS) of hyperspectral technology with optical grating (such as atmospheric infrared sounder AIRS) and interference (such as infrared atmospheric sounder interferometer IASI), the number of channels has increased from dozens to thousand even thousands. The first infrared hyperspectral atmospheric sounder on geostationary satellite, GIIRS (Geostationary Interferometric Infrared Sounder) with 1650 spectral channels is loaded on FY-4A meteorological satellite, which is China's second-generation geostationary meteorological satellite launched in December 2016. GIIRS is an interference spectrometer, covering the long-wave band 700–1130 cm^{-1} and the medium-wave band 1650–2250 cm^{-1}. Launched in November 2017, the polar-orbiting meteorological satellite FY-3D also carried an infrared hyperspectral atmospheric sounder named HIRAS with 1370 spectral channels, HIRAS covers three spectral bands, the long-wave band 650–1135 cm^{-1}, the medium-wave band I 1210–1750 cm^{-1} and the medium-wave band II 2155–2550 cm^{-1} (Dong et al., 2013; Zhang et al., 2017; Gong, 2018; Hua and Mao, 2018; Yang et al., 2018; Dai et al., 2019; Liu, 2019; Song et al., 2019).

The data of infrared hyperspectral atmospheric sounder has the horizontal spatial characteristics, whose formation mechanism is the same as imager. For example, horizontal spatial resolution of substellar point of FY-4A GIIRS is 16 km. More importantly, the infrared hyperspectral atmospheric sounding data has vertical spatial characteristics (VSC).

So far, there have been a few studies on the VSC related to the infrared hyperspectral atmospheric sounding, which mainly focus on the inversion products of atmospheric parameters rather than on the vertical sounding data. Zeng (1974) defined measurable altitude as altitude of the effective radiation layer and the vertical resolution as a discernible vertical scale depending on the effective information content of selected channels (Zeng, 1974). Conrath (1972) first applied the Backus-Gilbert method to satellite inversion and used the average weighting function to calculate the vertical resolution (Conrath, 1972). Thompson et al. (1976) and Newman (1979) found that in the field of satellite inversion, the Backus-Gilbert results could not reasonably reflect the true vertical resolution due to the frequent occurrence of negative average weighting functions (Thompson et al., 1976; Newman, 1979). Purser and Huang (1993) defined a method to calculate the effective data density of time observation data and verified that the method could reasonably describe the vertical resolution (Purser and Huang, 1993). Wang et al. (2007) and Maddy and Barnet (2008) analyzed the vertical resolution of AIRS and IASI products with effective data density method and HMFW (half max full width) method respectively (Wang et al., 2007; Maddy and Barnet, 2008). Dong et al. (2013) calculated the vertical resolution of atmospheric temperature and humidity profile observed by the FY-4A infrared hyperspectral resolution atmospheric sounder based on Backus-Gilbert method, effective data density method and HMFW method with the 1976 American standard atmosphere as the atmospheric state (Dong et al., 2013). Bao et al. (2017) simulated the GIIRS brightness temperature data and studied the atmospheric temperature inversion method of FY-4A satellite (Bao et al., 2017). There lacks the VSC analysis the hyperspectral sounding data itself.

Analyzing the VSC of hyperspectral sounding data is valuable, since the VSC of atmospheric parameter inversion products is the combined result of the VSC of atmospheric sounding data and the inversion method. Further, the direct assimilation is an important application approach of sounding data.

As shown in Table 1, different from the horizontal spatial characteristics of remote sensing data which are determined directly by the optical and scanning design of remote sensing instrument, the VSC of infrared hyperspectral atmospheric sounding data are determined indirectly by the design of spectral channels of the sounder, and its formation mechanism is relatively complex. It is related not only to the design of sounder, but also to the atmospheric parameter concerned. For different atmospheric parameters, the VSC may be different for the same sounder.

In this paper, we attempt to analyze systematically the formation mechanism of VSC of the infrared hyperspectral atmospheric sounding data. On this basis, we define the indicators of VSC and establish their mathematical models. These indicator models will be applied to evaluate the VSC of FY-4A GIIRS data for atmospheric temperature.

This research is helpful to deeply grasp the infrared hyperspectral sounding mechanism of the vertical distribution of atmospheric parameters, and to evaluate the data VSC of in-orbit and in-developing infrared hyperspectral atmospheric sounders, and provides basic information for analyzing the constitution of the VSC of

Table 1 Spatial characteristics of remote sensing data

Remote sensing instrument type	Spatial characteristic type	Formation mechanism	Research
Imager	horizontal spatial characteristic	direct and simple 1) Determined by instantaneous FOV and total FOV of the imager, and satellite orbital altitude 2) Independent of surface parameters	Mature
Sounder	horizontal spatial characteristics	Similar to imager	Mature
	Vertical spatial characteristics	Indirect and complex 1) Determined by spectral channels and their band coverage of the sounder 2) Related to the concerned atmospheric parameter and its markers	Few research

atmospheric inversion products. It is valuable for the application and further development of satellite infrared hyperspectral atmospheric sounding technology.

2 The VSC formation mechanism of infrared hyperspectral atmospheric sounding data

2.1 Atmospheric sounding equation

Assuming that the atmosphere is a plane parallel molecular layer in state of local heat balance, and the sounding band is medium-wave infrared band (excluding its molecular scattering segment) and long-wave infrared band, the radiation observed in the direction of substellar point is:

$$I_\nu = \int_{p_s}^{0} [B_\nu(T_p) - \varepsilon_{s\nu} B_\nu(T_s)] \frac{\mathrm{d}H_\nu(p)}{\mathrm{d}p} \mathrm{d}p + \varepsilon_{s\nu} B_\nu(T_s) + I'_{\nu-\mathrm{sun}} + \varepsilon'_\nu, \quad (1)$$

where I_ν is the radiation intensity measured by satellite sounder, and on the right side, the first item is the contribution of atmospheric radiation, the second item is the contribution of surface radiation through atmospheric transmission, the third item is the contribution of sunlight in the infrared band reflected by surface, the fourth item is the instrument error of sounder. ν is wavenumber, T_p is the temperature at pressure p, $B_\nu(T_p)$ is the blackbody radiation intensity at T_p, $H_\nu(p)$ is the transmittance from p to the top of atmosphere, $\varepsilon_{s\nu}$ is the surface emissivity, T_s is the surface temperature, $B_\nu(T_s)$ is the surface blackbody radiation intensity, p_s is the surface pressure, $H_\nu(p_s)$ is the transmittance from surface to the top of atmosphere.

Similar to the horizontal spatial characteristics of imaging data which concerns where the surface being looked at and doesn't concern at what extent the surface being seen clearly, the VSC of infrared sounding data is also defined to pay attention to where the atmosphere being looked at and doesn't pays attention to at what extent the atmosphere being seen clearly. That is, only the first of the four items on the right side of Eq. (1) need to be included for analyzing the VSC of infrared sounding data. The other three items of the four items on the right side of Eq. (1) will contribute to the VSC of the inversion products of infrared sounding.

Therefore, for infrared hyperspectral atmospheric sounder, if there are m channels and the central wavenumbers are ν_i $(i = 1,2,...,m)$, the equation used to analyze the VSC of sounding data is:

$$L_{\nu_i} = \left[\int_{p_s}^{0} B_{\nu_i}(T_p) - \varepsilon_{s\nu_i} B_{\nu_i}(T_s) \right] \frac{\mathrm{d}H_{\nu_i}(p)}{\mathrm{d}p} \mathrm{d}p, \quad (2)$$

where L_{ν_i} is the atmospheric radiation intensity. All the quantities in Eq. (2) related to wavenumber mean the average for bandwidth of spectral resolution centered at ν_i.

The altitude distribution of atmospheric temperature, water vapor, ozone (O_3), carbon dioxide (CO_2), methane (CH_4), nitrous oxide (N_2O) and other atmospheric absorption gases is reflected in L_{ν_i} by influencing atmospheric radiation and transmittance. It should be noted that the expression of an atmospheric parameter may be changed. For example, Li et al. do not use the mixing ratio q, but use the logarithm of the mixing ratio $\ln q$ for atmospheric water vapor (Li et al., 1994).

2.2 The response equations of atmospheric parameter variations

Supposing the altitude distribution of atmospheric temperature and atmospheric absorption gases are uniformly expressed by $a_j(p)$ $(j = 1,2,...,n)$, the change of satellite received radiation caused by the variations of atmospheric temperature and atmospheric absorbed gases can always be expressed in an approximate linear form as follows:

$$\delta L_{\nu_i} \approx \sum_{j=1}^{n} \int_{0}^{p_s} K_{ij}(p) \delta[a_j(p)] \mathrm{d}p \ (i = 1,2,...,m), \quad (3)$$

where $\delta[a_j(p)]$ is the variation of the jth atmospheric

parameter at p, $K_{ij}(p)$ is the response weighting function of the ith spectral channel for $\delta[a_j(p)]$. For an atmospheric parameter, if its expression is changed, the corresponding response weighting function will also be changed.

From Eq. (3), the change of radiation received by satellite sounder in a spectral channel consists of the variation effects of various atmospheric parameters. For the variations of different atmospheric parameters, their effective altitude ranges reflected in the sounder signal may be different. If the spectral channel is not the absorption channel of an atmospheric parameter, there is no response of this parameter at all in the sounder signal. Therefore, in contrast to the analysis of horizontal spatial characteristics which are derived from FOV design of imager and doesn't related to surface parameters, the analysis of VSC derived from the spectral channel design of sounder must make clear which atmospheric parameter is referred to.

According to Eq. (3), the signal response of the jth atmospheric parameter variation in the ith spectral channel is:

$$\delta L^j_{\nu_i} = \int_0^{p_s} K_{ij}(p)\delta[a_j(p)]\mathrm{d}p \ (i = 1,2,...,m, j = 1,2,...,n). \tag{4}$$

The VSC of atmospheric sounding data should not only specify which atmospheric parameter is interested in and what its expression form is defined, but also what meaning of its variation is specified. The variation of atmospheric parameter can be either absolute as shown in Eq. (3) or relative. The latter is the variation concerned by optimal selection of infrared hyperspectral atmospheric vertical sounding channels (Rodgers, 1996).

If we are concerned with relative variations of atmospheric parameters, that is,

$$\delta[b_j(p)] = \delta[a_j(p)]/\sqrt{\overline{\delta^2[a_j(p)]}} \ (j = 1,2,...,n), \tag{5}$$

Then, Eq. (4) can be rewritten as,

$$\delta L^j_{\nu_i} = \int_0^{p_s} W_{ij}(p)\delta[b_j(p)]\mathrm{d}p \ (i = 1,2,...,m, j = 1,2,...,n), \tag{6}$$

where

$$W_{ij}(p) = K_{ij}(p)\sqrt{\overline{\delta^2[a_j(p)]}}. \tag{7}$$

The altitude in above equations is expressed by pressure p. In fact, it can also be expressed by geometric height z. At this point, Eq. (4) and Eq. (6) can be rewritten as follows.

If the absolute variation of atmospheric parameter is concerned, and the geometric altitude is used as altitude parameter,

$$\delta L^j_{\nu_i} = \int_{z_{\mathrm{top}}}^{0} \left\{K_{ij}(p)\frac{\mathrm{d}p}{\mathrm{d}z}\right\}\delta\left[a_j(p)\right]\mathrm{d}z$$

$$(i = 1,2,...,m, j = 1,2,...,n). \tag{8}$$

If the relative variation of atmospheric parameter is concerned, and the geometric altitude is used as altitude parameter,

$$\delta L^j_{\nu_i} = \int_{z_{\mathrm{top}}}^{0} \left\{W_{ij}(p)\frac{\mathrm{d}p}{\mathrm{d}z}\right\}\delta\left[b_j(p)\right]\mathrm{d}z$$

$$= \int_{z_{\mathrm{top}}}^{0} \left\{K_{ij}(p)\sqrt{\overline{\delta^2[a_j(p)]}}\frac{\mathrm{d}p}{\mathrm{d}z}\right\}\delta\left[b_j(p)\right]\mathrm{d}z$$

$$(i = 1,2,...,m, j = 1,2,...,n). \tag{9}$$

We should note that unit of $K_{ij}(p)$ and $K_{ij}(p)\frac{\mathrm{d}p}{\mathrm{d}z}$ is "the unit of radiation change/(the unit of atmospheric parameter variation×the unit of altitude)," the unit of $W_{ij}(p)$ and $W_{ij}(p)\frac{\mathrm{d}p}{\mathrm{d}z}$ is "the unit of radiation change/the unit of altitude."

In conclusion, the equations for analyzing the VSC of atmospheric sounding data are Eqs. (4), (6), (8), and (9).

In practical application of Eqs. (4), (6), (8), and (9), it is always necessary to discretize the integration on altitude, that is, to stratify the atmosphere. Taking Eq. (4) as an example, if the atmosphere is stratified into layers ($l = 1,2,...,L^*$), the pressure difference, the average weighting function and the average atmospheric parameter variation of each layer are p_i, $K_{ij}(p_i)$, $\delta[a_j(p_i)]$ respectively, then the discretization form of Eq. (4) is as follows,

$$\delta L^j_{\nu_i} \approx \sum_{l=1}^{L^*} K_{ij}(p_l)\delta[a_j(p_l)]\ \Delta p_l$$

$$(i = 1,2,...,m, j = 1,2,...,n). \tag{10}$$

2.3 The response analysis of atmospheric parameter variations

Atmospheric temperature sounding is based on the absorption characteristics of atmospheric gases with known content of uniform altitude distribution (mixing ratio independent of altitude), such as CO_2 and O_2. The sounding of variable atmospheric absorption gases such as atmospheric water vapor and O_3 takes advantage of their own absorption characteristics. According to Kirchhoff's

law, the emissivity and absorptivity of any atmospheric component are equal, and the radiation received by satellite sounder contains atmospheric emissions at different altitudes which are weakened by the atmospheric absorption higher than emission altitude.

Therefore, for a certain atmospheric parameter $a_j(p)$ $(j = 1,2,...,n)$ expressed properly, as long as the ith channel ν_i $(i = 1,2,...,m)$ is the absorption channel of this parameter, there will be a special altitude where the variation of this parameter variation will be responded most sensitively by the ith channel compared to the variation of this parameter at other altitudes. That is, the weighting function is the largest at this special altitude.

Figure 1 shows the change of weighting function with geometric altitude for temperature relative change sounding applying spectral channels 720 cm^{-1}, 720.625 cm^{-1}, 790 cm^{-1}, 790.625 cm^{-1}, 791.25 cm^{-1}, 1048.125 cm^{-1}, 1651.875 cm^{-1}, 1748.75 cm^{-1} and 1771.25 cm^{-1}, and for water vapor mixing ratio relative change sounding applying spectral channels 1048.125 cm^{-1} and 1651.875 cm^{-1}, respectively.

From Fig. 1(a) and Fig. 1(b), it can be seen,

1) The weighting function of temperature relative change is positive, while the weighting function of water vapor mixing ratio relative change is negative.

2) The weighting function of an atmospheric parameter (including its expression and variation definition) is a continuous function. The variation of the weighting function with altitude corresponding the ith spectral channel and the jth atmospheric parameter reflects the VSC of the ith channel in response to the variation of the altitude distribution of the jth parameter.

Since the weighting function is related to the expression form of atmospheric parameter, we can and should, adopt an appropriate expression form so that the curve of weighting function change with altitude shows mainly a single peak or monotone characteristic.

3) The weighting functions of different atmospheric parameters are different in their altitude positions, altitude range sizes and shapes. Taking sounding channels 1048.125 cm^{-1} and 1651.875 cm^{-1} as examples, the shape and peak position of the weighting function change with altitude for temperature are different from that for water vapor.

In a word, the VSC of infrared hyperspectral atmospheric sounding data are determined by: 1) spectral coverage and spectral channel setting, 2) the atmospheric parameter interested, its expression form and meaning of variation. So, the formation mechanism of the VSC of infrared hyperspectral atmospheric sounding data is completely different from that of horizontal spatial characteristics of imaging data.

For an atmospheric parameter, if its expression form and the meaning of variation are specified, the variation information of this atmospheric parameter obtained by a spectral channel depends on the corresponding weighting function. The larger the weighting function is, the more variation information will be. The position, the main size and shape of weighting function curve determine the response of the atmospheric parameter variation in the spectral channel's signal, thus forms the VSC of sounding data obtained by this channel. With the change of the spectral channel, the position, the main size and shape of weighting function curve also change, so the channel's spectral coverage determines the vertical coverage of atmospheric parameter sounding.

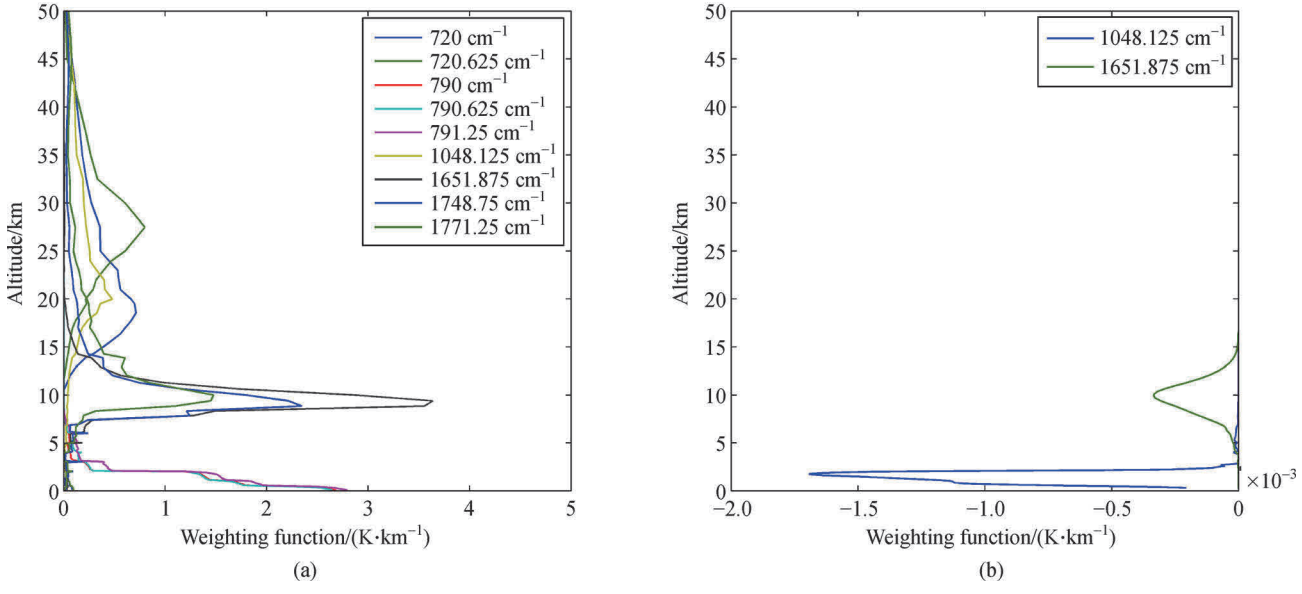

Fig. 1 (a) Temperature weighting functions and (b) water vapor weighting functions.

3 The VSC indicators and their mathematical models of infrared hyperspectral atmospheric sounding data

3.1 Characteristic indicators

As described in Section 1, the horizontal spatial characteristics of imaging data are usually characterized by pixel position, pixel position, pixel shape and the whole ground coverage of all pixels.

For the infrared hyperspectral atmospheric sounding data, the peak altitude of weighting function curve determines at what altitude the signal response of spectral channel to the variation of atmospheric parameter reaches maximum. The "bandwidth" of the weighting function curve determines to what extent the signal response of spectral channel can reflect the detailed vertical structure of atmospheric parameters. The asymmetry of the weighting function curve relative to the peak position determines the relative strength of the signal response of spectral channel due to the parameter variation in upper atmosphere and that in lower atmosphere. The vertical sounding coverage of atmospheric parameter is determined by the moving of weighting function curve with change of spectral channel in the whole range of sounding waveband. Therefore, similar to the horizontal spatial characteristics, the following four indicators can be used to characterize the VSC of infrared hyperspectral atmospheric sounding data for a certain atmospheric parameter including its definitions of expression and variation:

1) Sounding altitude

It reflects the altitude position of the response weighting function curve of a spectral channel. This indicator is corresponding to the imaging pixel position in the horizontal spatial characteristics of imaging data. The latter usually refers to the ground position pointed by the central axis of the instantaneous FOV of imager.

2) Sounding altitude resolution

It reflects the altitude range covered by the response weighting function curve of a spectral channel. This indicator is corresponding to the imaging pixel size due to the instantaneous FOV of imager. However, unlike imaging pixel size, which has a clear ground boundary, the weighting function curve is a gradient curve without a clear altitude boundary.

3) Sounding vertical asymmetry

It reflects the shape of the response weighting function curve with altitude of a spectral channel. This indicator is corresponding to the imaging pixel asymmetry relative to the imaging pixel position. At the substellar ground, the ground pixel observed by imager are symmetric. As the pixel gradually leaves from substellar toward a direction, it also gradually deviates in the same direction relative to the ground position pointed by the central axis of the instantaneous FOV of imager.

4) Sounding vertical coverage

It reflects combined altitude coverage of the response weighting functions of all spectral channels. This indicator is corresponding to the total ground range observed by imager.

3.2 Mathematical models

In the following paragraphs, h and $Q_{ij}(h)$ are used uniformly to represent altitude and response weighting function in Eqs. (4), (6), (8), and (9).

For a given spectral channel, with appropriate expression and variation definition of interested atmospheric parameter, the change of weighting function with altitude generally has the following features: 1) increase first and then decrease; 2) increase monotonically; 3) decrease monotonically. The latter two features can also be regarded as special cases of the first feature in the case of upper boundary (h_{top}) cutoff and that of lower boundary (h_{ground}) cutoff (see Fig. 2).

1) Sounding altitude

The mathematical model for sounding altitude is defined as the peak altitude of weighting function $h_{\max}$, that is

$$Q_{ij}(h_{\max}) = \max_{h_{\text{ground}} \leqslant h \leqslant h_{\text{top}}} [Q_{ij}(h)], \tag{11}$$

where

a) if $h_{\text{ground}} < h_{\max} < h_{\text{top}}$, $h_{\max}$ is in the concerned atmosphere;

b) if $h_{\max} = h_{\text{top}}$, $h_{\max}$ is at the upper boundary;

c) if $h_{\max} = h_{\text{ground}}$, $h_{\max}$ is at the lower boundary.

2) Sounding altitude resolution

The mathematical model of sounding altitude resolution is defined as the full width half max (FWHM) of the weighting function $Q_{ij}(z)$.

If h_{+50}, h_{-50} are respectively the upper and lower altitude corresponding to half max of weighting function (see Fig. 2), then

$$\begin{aligned} \text{FWHM} &= (h_{u5} - h_{d5}) \\ &= (h_{u5} - h_{\max}) + (h_{\max} - h_{d5}), \end{aligned} \tag{12}$$

where

$$h_{u5} = \min(h_{\text{top}}, h_{+50}), \quad h_{d5} = \max(h_{\text{ground}}, h_{-50}). \tag{13}$$

In Eq. (12), if the weighting function at the upper or lower atmospheric boundary is greater than half max of weighting function, then the atmospheric boundary ought to be taken as the cut-off altitude in the determination of sounding altitude resolution.

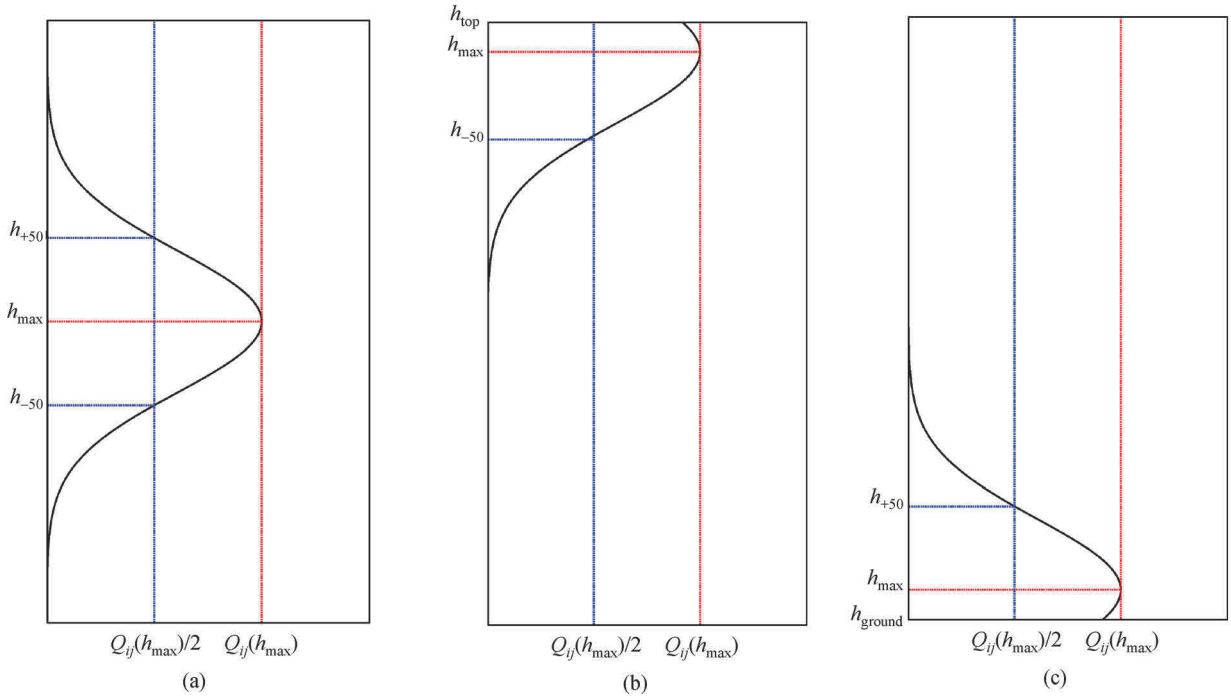

Fig. 2 Schematic diagram of weighting function.

3) Sounding vertical asymmetry

The mathematical model of sounding vertical asymmetry is defined as the ratio of the average of h_{u5} and h_{d5} minus $h_{\max}$ to FWHM, called skewness (SK for short).

$$SK = \frac{(h_{u5}+h_{d5})/2-h_{\max}}{h_{u5}-h_{d5}}. \tag{14}$$

If $SK=0$, the responses of parameter variation for atmosphere above the sounding height and that below the sounding height are same. If $SK>0$, the sounding is upper skewness, that is, the responses of parameter variation for atmosphere above the sounding height is stronger than that below the sounding height. The larger the SK, the more obvious the upper skewness. If $SK<0$, the sounding is lower skewness, that is, the responses of parameter variation for atmosphere above the sounding height is weaker than that below the sounding height. The smaller the SK, the more obvious the lower skewness.

4) Sounding vertical coverage

The mathematical model of the sounding vertical coverage of an infrared band is defined as the combination of altitude range between the upper and the lower 50% peak response altitude for all spectral channels, that is,

$$\mathrm{R} = \bigcup_{h_{\text{ground}}\leqslant h\leqslant h_{\text{top}}} [h_{d5},h_{u5}]. \tag{15}$$

If there are several infrared sounding bands, the total vertical coverage of sounding data is the union of the sounding vertical coverages of these bands.

4 The evaluation of VSC for atmospheric temperature sounding with FY-4A GIIRS data

4.1 FY-4A GIIRS technical parameters and the calculation of response weighting function for atmospheric temperature variation

The FY-4A GIIRS scanning system performs a step-resident scan in the east–west and north–south directions, selecting the desired area to collect the atmospheric radiation signal. It uses the interference spectroscopy technology and covers the long-wave infrared band 700–1130 cm^{-1} and the medium-wave infrared band 1650–2250 cm^{-1}, with the spectral resolution of 0.625 cm^{-1}. There are 1650 spectral channels in total, including 689 long-wave channels and 961 medium-wave channels. There have three working modes: sounding mode, calibration mode and pointing mode. The sounding mode includes full disk sounding, regional sounding (5000 km × 5000 km), meso-small scale sounding (1000 km × 1000 km), and solar avoidance. The calibration mode includes star sensing calibration, blackbody calibration, cold space calibration and spectral calibration. The substellar spatial resolution is 16 km, the radiometric calibration accuracy is 1.5 K, the spectral calibration accuracy is 10 ppm, and the time resolution can be as high as 35 min for meso-small scale sounding (Hua and Mao, 2018).

Atmospheric temperature is taken as the interested sounding parameter and its relative variation is concerned.

The radiation change received by satellite sounder is expressed by the difference of equivalent blackbody temperature, and the altitude is expressed by geometric altitude.

The response weighting function of the ith spectral channel for the variation of the jth atmospheric parameter, $Q_{ij}(h) \equiv K_{ij}(p)\sqrt{\overline{\delta^2[a_j(p)]}}\frac{\mathrm{d}p}{\mathrm{d}z}$, can be calculated by the line-by-line radiative transfer model (LBLRTM). The statistical average profile and standard deviation profile of vertical distribution of atmospheric temperature are as input (Luo and Yin, 2019) are applied as the input of LBLRTM. The atmosphere 0–100 km is divided into 121 layers for running LBLRTM. The weighting function of each layer is obtained by taking the relative variation of this layer's temperature as 1 while keeping all other layers' temperature unchanged. We focus on the atmosphere below the stratopause (about 50 km high), in which the water vapor, O_3, CO_2 and other absorbing gases are mainly distributed.

Since the atmosphere is divided into layers, the judgment of sounding altitude should include the influence of atmospheric discretization. Here, $h_{\max}$ is used to express the model nominal sounding altitude, and $(h_{\max}-a,\ h_{\max}+b)$ is used to express the actual sounding altitude. Where, a and b are respectively 50% width of the adjacent lower and upper layers.

4.2 Sounding altitude

Figure 3 shows the sounding altitude distribution of the 689 channels in long-wave band and the 961 channels in medium-wave band of FY-4A GIIRS. The statistical results of sounding altitude distribution are given in Fig. 4 and Table 2.

It can be seen from Figs. 3 and 4 and Table 2,

1) The sounding altitudes of long-wave band (700–1130 cm^{-1}) channels are distributed near 16 altitudes, while the sounding altitudes of medium-wave band (700–1130 cm^{-1}) channels are distributed near 15 altitudes. There is no peak response above 30 km.

2) Among the 689 channels in the long-wave band, there are 589 channels with sounding altitude of 1 km or less accounting for 85.5%, 85 channels with sounding altitude of (1 km, 7 km] accounting for 13.1% and only 4 channels with peak altitude of (7 km, 9 km]. The sounding altitudes of the remaining 6 channels are between 16–29 km.

3) Among the 961 channels in the medium-wave band, there are 349 channels with sounding altitude of 1km or less accounting for 36.3%, 420 channels with sounding altitude of (1 km, 6 km] accounting for 43.7%, 187 channels with sounding altitude of (6 km, 11 km] accounting for 19.6%. The sounding altitudes of the remaining 3 channels are between 13 km and 14 km.

4.3 Sounding altitude resolution

Figures 5 and 6 show the distribution and cumulative distribution of sounding altitude resolution of FY-4A GIIRS spectral channels.

It can be seen from Figs. 5 and 6,

1) For long-wave channels, there are 606 channels with sounding altitude resolution better than 2 km (included) accounting for 88%, 35 channels with sounding altitude resolution within (2 km, 3 km] accounting for 5.1% and 17 channels with sounding altitude resolution within (3 km,

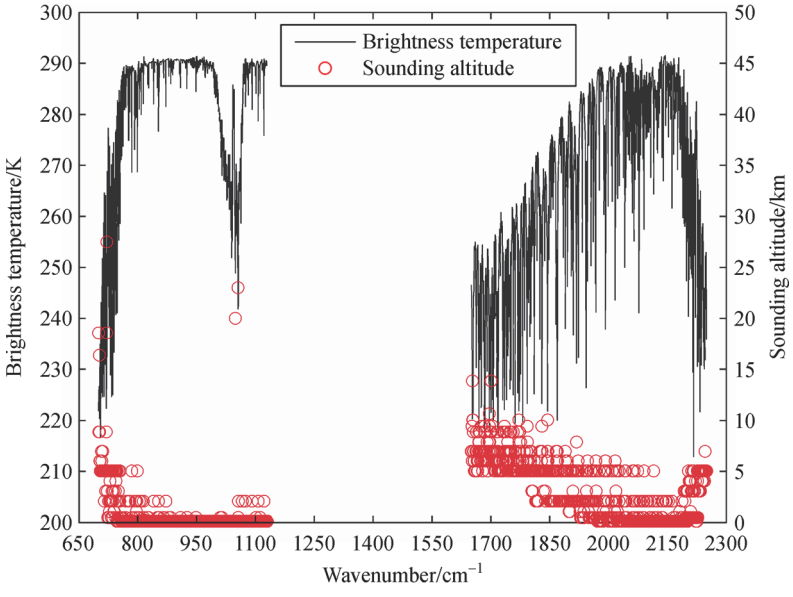

Fig. 3 Temperature sounding altitude distribution of FY-4A GIIRS spectral channels.

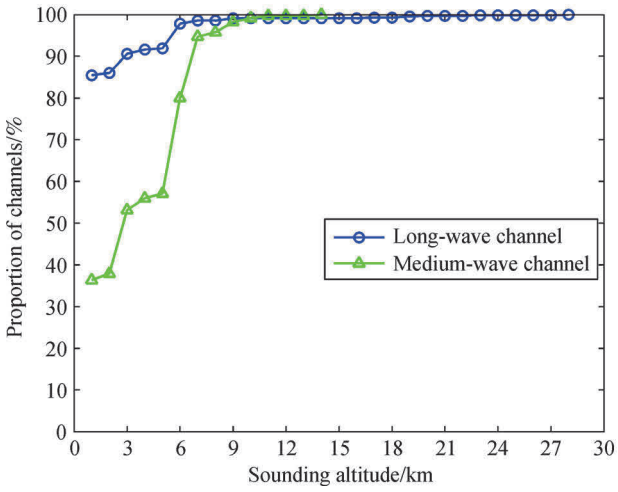

Fig. 4 Cumulative temperature sounding altitude distribution of FY-4A GIIRS spectral channels.

4 km] accounting for 2.5%. The sounding altitude resolutions of remaining 31 channels are worse than 4 km accounting for 4.5%.

2) For medium-wave channels, there are 750 channels with sounding altitude resolution better than 2 km (included) accounting for 78%, 122 channels with sounding altitude resolution within (2 km, 3 km] accounting for 12.7% and 46 channels with sounding altitude resolution within (3 km, 4 km] accounting for 4.8%。The sounding altitude resolutions of remaining 43 channels are worse than 4 km accounting for 4.5%.

The average and standard deviation of sounding altitude resolution varying with sounding altitude are shown in Fig. 7.

Overall, it can be seen from Figs. 7(a) and 7(b), as the sounding altitude rises, the average sounding altitude resolution tends to be worse gradually. The average sounding altitude resolution of medium-wave channels is basically better than that of long-wave channels. The dispersion of sounding altitude resolution does not show regularity.

4.4 Sounding vertical asymmetry

The distribution of sounding vertical asymmetry of FY-4A GIIRS spectral channels vs. sounding altitudes is shown in Fig. 8. The sounding asymmetry of channels with sounding altitude below 2 km is all upper-skewness, the spectral channel responses of other sounding altitudes may be upper-skewness or lower-skewness. This is completely different from the monotone variation of pixel asymmetry in an imager when the pixel deviates from the substellar position.

4.5 Sounding vertical coverage

The distribution of upper and lower altitudes where the response weighting function reaches half of peak response, h_{u5} and h_{d5}, with sounding altitude is shown in Fig. 9.

It can be seen from Fig. 9.

1) Most spectral channels of FY-4A GIIRS are sensitive to the temperature variation in troposphere.

Table 2 The number of spectral channels for different sounding altitude in long-wave band and medium-wave band of FY-4A GIIRS

Long-wave band				Medium-wave band			
No.	Model nominal h_{max} /km	Actual h_{max} /km	Number of channels	No.	Model nominal h_{max} /km	Actual h_{max} /km	Number of channels
1	0.11	(0.05, 0.14)	552	1	0.11	(0.05, 0.14)	251
2	0.17	(0.14, 0.20)	1	2	0.47	(0.41, 0.53)	98
3	0.47	(0.41, 0.53)	36	3	1.04	(0.98, 1.10)	15
4	1.04	(0.98, 1.10)	4	4	2.05	(1.99, 2.08)	147
5	2.05	(1.99, 2.08)	31	5	3.05	(3.00, 3.10)	27
6	3.05	(3.00, 3.10)	7	6	4.03	(3.97, 4.05)	11
7	4.03	(3.97, 4.05)	2	7	5.03	(4.99, 5.06)	220
8	5.03	(4.99, 5.06)	41	8	6.02	(5.98, 6.11)	71
9	6.02	(5.98, 6.11)	3	9	6.96	(6.92, 7.18)	70
10	6.96	(6.92, 7.18)	2	10	7.86	(7.63, 8.10)	10
11	8.87	(8.61, 9.14)	4	11	8.87	(8.61, 9.14)	24
12	16.36	(15.80, 16.70)	1	12	9.41	(9.14, 9.72)	9
13	18.56	(18.16, 19.05)	2	13	10.03	(9.72, 10.34)	4
14	20.00	(19.77, 20.50)	1	14	10.65	(10.34, 10.99)	1
15	23.00	(22.50, 23.50)	1	15	13.87	(13.39, 14.07)	3
16	27.50	(26.25, 28.75)	1				

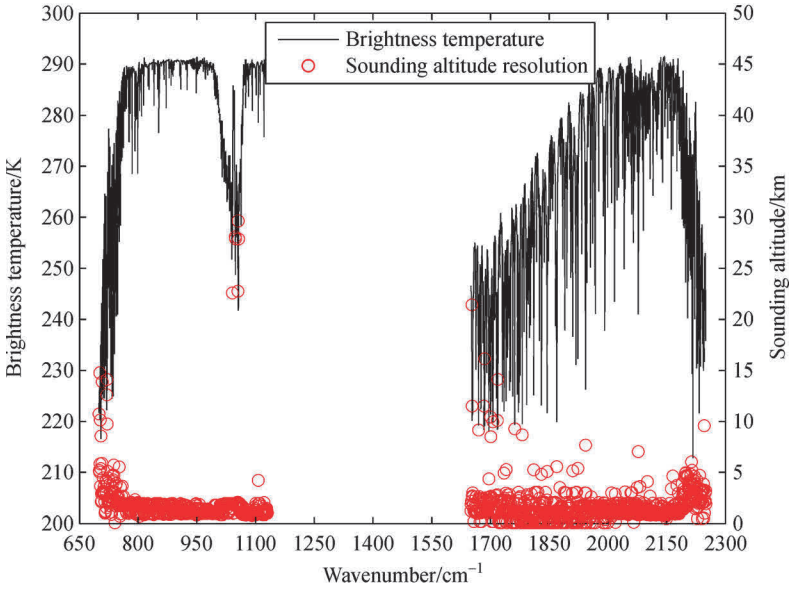

Fig. 5 Temperature sounding altitude resolutions of FY-4A GIIRS spectral channels.

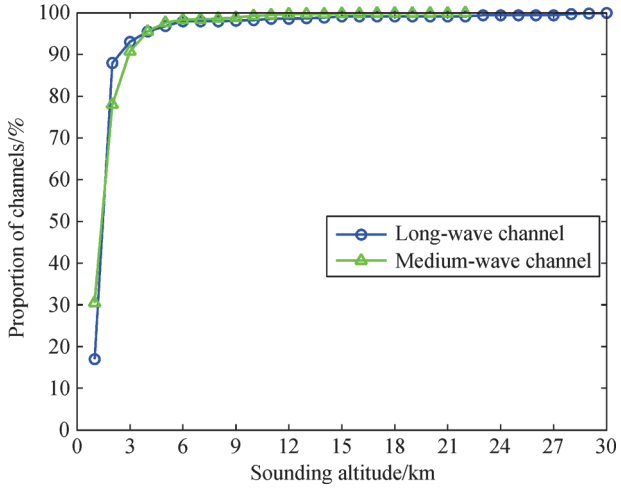

Fig. 6 Cumulative distribution of temperature sounding altitude resolution of FY-4A GIIRS spectral channels.

2) There are 9 spectral channels sensitive to the temperature variation in lower stratosphere from 14–29 km.

3) Due to the maximum sounding altitude of FY-4A GIIRS for atmospheric temperature is below 30 km, the temperature variation above 35 km can't be sounded by FY-4A GIIRS.

5 Conclusions

In this paper, focused on the VSC of satellite infrared hyperspectral atmospheric sounding data, the formation mechanism of VSC is analyzed, the mathematical models of VSC indicators are established, and the VSC of FY-4A GIIRS data for atmospheric temperature sounding is evaluated.

The VSC of sounding data and the horizontal spatial characteristics of imaging data both concern about where the remote sensing instruments look at, but not about whether the target can be seen clearly, which is answered by data inversion.

The difference between VSC and horizontal spatial characteristic is mainly that:

1) The latter is determined directly by the instantaneous FOV and total FOV of imager and the height of satellite, while the former is determined indirectly by the spectral channel distribution and wave band coverage of sounder.

2) The latter is independent of which surface parameter is interested, while the former is related to which atmospheric parameter is interested. In addition, the VSC is also related to the expression and variation definitions of atmospheric parameter.

Four VSC indicators and their mathematical models are proposed, which include the sounding altitude, the sounding altitude resolution, the sounding vertical asymmetry and the sounding vertical coverage.

The VSC of FY-4A GIIRS data are evaluated with the relative variation of atmospheric temperature as sounding target. The results are:

1) The sounding altitudes of spectral channels in the long-wave band are mostly lower than 9 km, and there are 6 channels whose corresponding sounding altitudes are in 16–29 km. The sounding altitudes of spectral channels in the medium-wave band are all in the troposphere (<14 km).

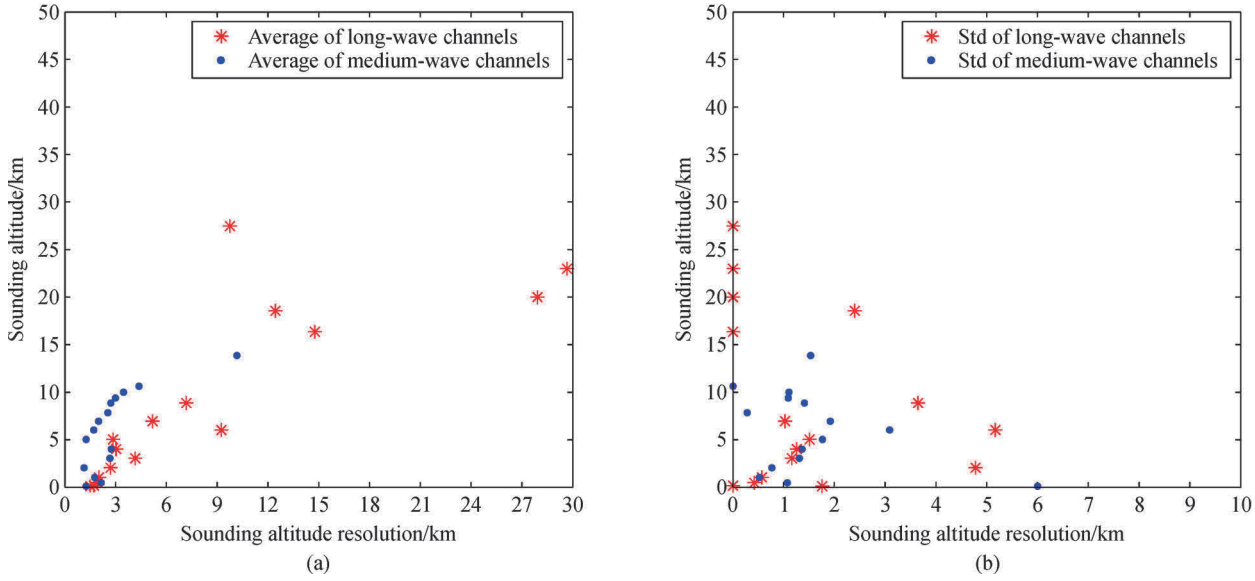

Fig. 7 Vertical distribution of (a) average and (b) standard deviation of temperature sounding altitude resolution of FY-4A GIIRS spectral channels.

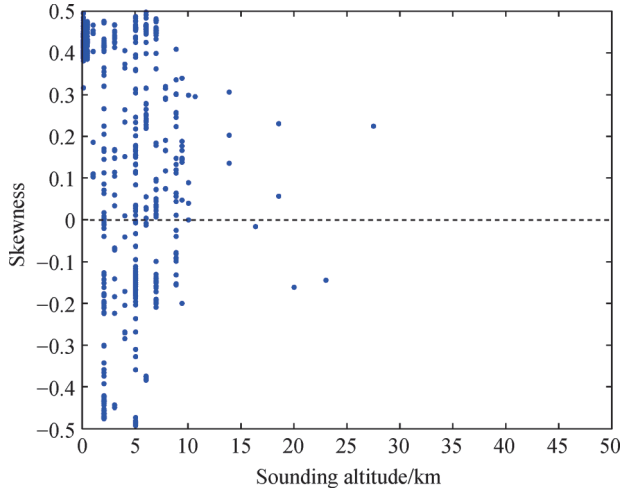

Fig. 8 Temperature sounding vertical asymmetry of FY-4A GIIRS spectral channels.

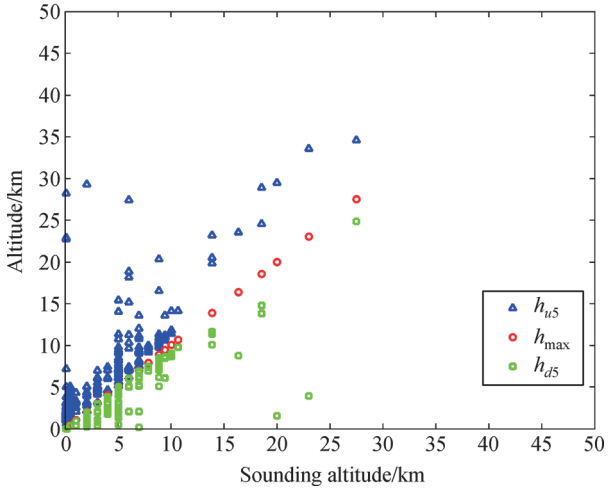

Fig. 9 Temperature sounding vertical coverage of FY-4A GIIRS spectral channels.

2) The sounding altitude resolutions of spectral channels are mostly better than 2 km (included) accounting for 88% in the long-wave band and 78% in the medium-wave band, respectively.

3) For most sounding altitudes except for near surface, the sounding vertical asymmetries of spectral channels may be either positive or negative.

4) The sounding vertical coverage of spectral channels is from ground to 35 km. There is no coverage above 35 km.

For further research, we will evaluate the VSC of other atmospheric parameters such as water vapor and ozone, and compare their features.

References

Bao Y S, Wang Z J, Chen Q, Zhou A M, Dong Y H, Min J Z (2017). Preliminary study on atmospheric temperature profiles retrieval from GIIRS based on FY-4A satellite. Aerospatial Shanghai, 34: 28–37

Conrath B J (1972). Vertical resolution of temperature profiles obtained from remote radiation measurements. J Atmos Sci, 29(7): 1262–1271

Dai L Q, Tang S F, Xu L N, Sun Q Y, Yang X B, Wang Z M, Jin Z L, Zhao Y H (2019). Development overview of spatial-borne multi-spectral imager with band range from visible to thermal infrared. Infrared Technology, 41(2): 107–117

Dong C H, Li J, Zhang P, Wu C Q, Qi C L, Yao Z G, Wu X B, Li B,

Zheng J, Liu H, Lu Q F, Ma G, Bai W G, Jiang D M, Zhang Y (2013). Principle and Application of Satellite Hyper-spectral Infrared Atmospheric Remote Sensing. Beijing: Science Press (in Chinese)

Friedl M A, Mciver D K, Hodges J C F, Zhang X Y, Muchoney D, Strahler A H, Woodcock C E, Gopal S, Schneider A, Cooper A, Baccini A, Gao F, Schaaf C (2002). Global land cover mapping from MODIS: algorithms and early results. Remote Sens Environ, 83(1–2): 287–302

Gong R (2018). GaoFen 5 satellite. Satellite Application, 77(05):76

Hu X Q, Niu X H, Xu N, Wu R H, Ding L, Yang Z D, Zhang P (2018). Improvement and application ability promotion of FY-3D medium-resolution spectral imager II. In: 35th Annual Meeting of China Meteorological Society

Hua J W, Mao J H (2018). Atmospheric vertical sounder on FY-4 meteorological satellite. Science Frontier, 70(1): 24–29

Li J, Zhou F X, Zeng Q C (1994). Simultaneous non-linear retrieval of atmospheric temperature and absorbing constituent profiles from satellite infrared sounder radiances. Adv Atmos Sci, 11(2): 128–138

Liu W Q (2019). “Gaofen 5 satellite payload development” album. J Atmosph Environ Opt, 14(01): 5 (in Chinese)

Luo S, Yin Q (2019). Statistical characteristics analysis of global temperature vertical profile. J Trop Meteorol, 35(4): 556–566

Maddy E S, Barnet C D (2008). Vertical resolution estimates in Version 5 of AIRS operational retrievals. IEEE Trans Geosci Remote Sens, 46 (8): 2375–2384

Niclòs R, Valiente J A, Barberà M J, Caselles V (2014). Land surface air temperature retrieval from EOS-MODIS images. IEEE Geosci Remote Sens Lett, 11(8): 1380–1384

Newman W I (1979). The application of generalized inverse theory to the recovery of temperature profiles. J Atmos Sci, 36(4): 559–565

Purser R J, Huang H L (1993). Estimating effective data density in a satellite retrieval or an objective analysis. J Appl Meteorol, 32(6): 1092–1107

Qi C L, Gu M J, Hu X Q, Wu C (2016). FY-3 satellite infrared high spectral sounding technique and potential application. Advanced in Meteorological Science and Technology, 6(1): 88–93

Qi C L, Zhou F, Wu C Q, Hu Q, Gu M J (2019). Spectral calibration of Fengyun-3 satellite high-spectral resolution infrared sounder. Optics and Precision Engineering, 27(4): 747–755

Rodgers C D (1996). Information content and optimization of high spectral resolution remote measurements. Advances in Spatial Research, 21(97): 136–147

Song C, Yin Q, Xie Y N (2019). Development of channel selection methods for infrared atmospheric vertical sounding. Infrared, 40(6): 18–26

Thompson O E, Eom J K, Wagenhofer J R (1976). On the resolution of temperature profile fine structure by the NOAA satellite vertical temperature profile radiometer. Mon Weather Rev, 104(2): 117–126

Wang F, Li J, Schmit T J, Ackerman S A (2007). Trade-off studies of a hyperspectral infrared sounder on a geostationary satellite. Appl Opt, 46(2): 200–209

Yang Y H, Yin Q, Shu J (2018). Channel selection of atmosphere vertical sounder (GIIRS) onboard the FY-4A geostationary satellite. J Infrared Millim W, 37(5): 603–610

Zhang Z Q, Lu F, Fang X, Tang S H, Zhang X H, Xu Y L, Han W, Nie S P, Shen Y B and Zhou Y Q (2017). Application and development of the FY-4A meteorological satellite. Aerospatial Shanghai, 34(4): 8–19

Zeng Q C (1974). Principle of Atmospheric Infrared Telemetry. Beijing: Science Press, 13–30

AUTHOR BIOGRAPHIES

Ci SONG is a post-doctor of School of Communication and Information Engineering, Shanghai University and lecturer of College of Science, Zhongyuan University of Technology. She received her B.S. degree in mathematics and applied mathematics from Henan Normal University in 2008, M.S. degree in mathematics and applied mathematics from East China Normal University and Ph.D degree in physical geography from East China Normal University. Her research interests include remote sensing information processing and application, remote sensing mechanism and radiation transmission.

Qiu YIN is a Research Professor of Shanghai Meteorological Service, China Meteorological Administration (CMA). He received his B.S. and M.S. degrees in atmospheric physics from Nanjing University and Ph.D degree in physical electronics from Shanghai Institute of Technical Physics, Chinese Academy of Sciences (CAS). His research interests include atmospheric radiation transfer model, remote sensing information processing and environmental remote sensing application. He has published 2 national standards and more than 100 academic papers.